ISSN 0915-633X

NATIONAL INSTITUTE FOR FUSION SCIENCE

Variational Approach to a Turbulent Swirling Pipe Flow with the Aid of Helicity

A. Yoshizawa, N. Yokoi, S. Nisizima, S.-I. Itoh and K. Itoh

(Received - Jan. 18, 2001)

NIFS-680 Feb. 2001

RESEARCH REPORT
NIFS Series

TOKI, JAPAN

Variational approach to a turbulent swirling pipe flow with the aid of helicity

Akira Yoshizawa, Nobumitsu Yokoi, Shoiti Nisizima

Institute of Industrial Science, University of Tokyo, Komaba, Meguro-ku, Tokyo 153-8505, Japan

Sanae-I. Itoh,

Research Institute for Applied mechanics, Kyushu University 87, Kasuga, Fukuoka 816-8580, Japan

Kimitaka Itoh

National Institute for Fusion Science, Toki, Gifu 509-5292, Japan

Abstract

A turbulent swirling flow in a circular pipe is studied with the aid of a variational method. The turbulent-energy production effect, which is linked with spatial velocity gradients, expresses the energy cascade from mean to turbulent components of motion and is a cause of the loss of distinct mean-flow structures. In the turbulent-energy equation, weakening of the production effect tends to enhance the diffusion effect of turbulent energy, which is also harmful to the sustainment of such structures. An optimum state in which these two effects are reconciled with each other is sought with resort to a variational approach combined with helicity. The resulting state is expressed by the mean vorticity proportional to its curl. On this basis, the centerline axial vorticity is shown to play a central role in the occurrence of axial-velocity retardation or reversal in a turbulent swirling pipe flow.

Keywords: turbulent swirling flow, variational method, helicity, turbulent-energy production, reversal of pipe flow

I. INTRODUCTION

One of prominent features of turbulent flows is the enhancement of mixing effect. The feature may be typically seen in a turbulent circular-pipe flow. The enhanced mixing effect changes the flow structure from an elongated (parabolic) velocity profile in a laminar state to a flattened mean-velocity profile. This fact indicates that flow structures with large mean spatial velocity gradients, in general, tend to be smoothed out and lost in a turbulent flow.

A typical flow that keeps their intrinsic structures against turbulent mixing effect is a swirling flow in a circular pipe.[1] In the flow, swirl motion is imposed on the axial flow at the entrance of a pipe. Far downstream, this flow relaxes to a usual pipe flow with its axial component as a sole mean velocity. In the intermediate region subject to swirling effect, a characteristic feature of the flow is the retardation of an axial velocity near the centerline. With the increase in the entrance swirl intensity, the velocity near the axis is further retarded, eventually resulting in the reversal of flow direction.

The occurrence of such retarded or reversed flow structures results in large mean velocity gradients, compared with the nonswirling case. This fact suggests the existence of some mechanism under which those structures may survive against the turbulent mixing effect represented typically by the turbulent viscosity. The study of a swirling pipe flow is an interesting theme from a viewpoint of elucidating a coexistence mechanism of distinct mean-flow structures and fluctuations.

A swirling pipe flow is also a challenging subject for the test of the capability of turbulence models that are a useful tool in the analysis of engineering turbulent flows at high Reynolds numbers. Turbulent-viscosity models represented by the standard $K-\varepsilon$ model, in which the Reynolds stress is linear in the mean velocity-strain tensor, may capture the enhancement of mixing effect by fluctuations. Turbulent mixing effect generally contributes to the rapid loss of distinct mean-flow structures associated with the retardation and reversal of an axial velocity. In order that the $K-\varepsilon$ model may reproduce the results consistent with the observation of a swirling flow, the magnitude of the turbulent viscosity associated with the swirl component of mean velocity needs to be reduced to about one percent of its axial-component counterpart.[2] The range of applicability of turbulence models has been much enlarged through explicit algebraic[3-8] and second-order[9,10] models, but those models still cannot properly analyze a swirling pipe flow (see Ref. 11 for the attempt based on a second-order model).

In this work, we adopt an approach entirely different from the standard turbulence modeling, that is, a variational approach, and explore a coexistence mechanism of a mean-flow structure with large velocity gradients and fluctuations in a swirling pipe flow. Here we should stress that the purpose of this work is not to propose a substitute of current turbulence models, but to shed light on fundamental aspects of a mechanism missing from these models, as a first step towards their improvement.

This article is organized as follows. The fundamental equations and their related conservation property are given in Sec. II. In Sec. III, the variational approach to a turbulent flow with nonvanishing mean-flow helicity is developed, and a vorticity equation is derived. In Sec. IV, the solution of the vorticity equation is applied to a swirling pipe flow, and the reversed centerline velocity is discussed in comparison with observations. Reference is also made to a turbulent flow in an axially rotating pipe and the relationship with turbulence modeling. The concluding remarks are given in Sec. V.

II. FUNDAMENTAL EQUATIONS

A. Navier-Stokes equation and related conservation law

The Navier-Stokes equation for a viscous incompressible fluid is given by

$$\frac{\partial \mathbf{u}}{\partial t} + (\mathbf{u} \cdot \nabla)\mathbf{u} = -\nabla p + \nu \Delta \mathbf{u}, \tag{1}$$

with the solenoidal condition $\nabla \cdot \mathbf{u} = 0$. Here $\mathbf{u}$ is the velocity, p is the pressure divided by constant density, ν is the kinematic viscosity, and $\Delta = \nabla^2$.

The vorticity

$$\boldsymbol{\omega} = \nabla \times \mathbf{u} \tag{2}$$

obeys

$$\frac{\partial \boldsymbol{\omega}}{\partial t} = \nabla \times (\mathbf{u} \times \boldsymbol{\omega}) + \nu \Delta \boldsymbol{\omega}. \tag{3}$$

In relation to the first term on the right-hand side, we have the well-known relationship

$$\frac{|\mathbf{u} \times \boldsymbol{\omega}|^2}{|\mathbf{u}|^2 |\boldsymbol{\omega}|^2} + \frac{|\mathbf{u} \cdot \boldsymbol{\omega}|^2}{|\mathbf{u}|^2 |\boldsymbol{\omega}|^2} = 1. \tag{4}$$

Equation (4) indicates that larger $|\mathbf{u}\cdot\boldsymbol{\omega}|$ tends to give smaller $|\mathbf{u}\times\boldsymbol{\omega}|$. The decrease in $\nabla\times(\mathbf{u}\times\boldsymbol{\omega})$ leads to weakening of the energy cascade, which suggests that $\mathbf{u}\cdot\boldsymbol{\omega}$, which is called the helicity, is a candidate of a parameter controlling the sustainment of distinct flow structures in turbulence. This point is a motivation of the present work on a swirling flow.

The helicity $\mathbf{u}\cdot\boldsymbol{\omega}$ obeys[12,13]

$$\frac{\partial}{\partial t}\mathbf{u}\cdot\boldsymbol{\omega} = -2\nu\frac{\partial u_j}{\partial x_i}\frac{\partial \omega_j}{\partial x_i} + \nabla\cdot\left(-(\mathbf{u}\cdot\boldsymbol{\omega})\mathbf{u} + \left(-p+\frac{\mathbf{u}^2}{2}\right)\boldsymbol{\omega} + \nu\nabla(\mathbf{u}\cdot\boldsymbol{\omega})\right). \tag{5}$$

The integration of Eq. (5) in a whole fluid region V results in

$$\frac{\partial}{\partial t}\int_V \mathbf{u}\cdot\boldsymbol{\omega}dV = -\int_V 2\nu\frac{\partial u_j}{\partial x_i}\frac{\partial \omega_j}{\partial x_i}dV$$

$$+\int_S \mathbf{n}\cdot\left(-(\mathbf{u}\cdot\boldsymbol{\omega})\mathbf{u} + \left(-p+\frac{\mathbf{u}^2}{2}\right)\boldsymbol{\omega} + \nu\nabla(\mathbf{u}\cdot\boldsymbol{\omega})\right)dS, \tag{6}$$

from the Stokes integral theorem. Here S is the surface of V, and $\mathbf{n}$ is the outward unit vector normal to S. In Eq. (6), the second term on the right-hand side expresses the flux of helicity across S. Then a total amount of helicity in the absence of ν is conserved so long as there is no flux of helicity across S, entirely the same as for kinetic energy. This fact indicates that helicity is a quantity deserving much attention.

Let us simply see the structure of Eq. (6) in the light of the swirl motion at the entrance of a pipe. The vorticity arising the swirl motion is in the axial direction, which is combined with the axial velocity to generate helicity. Then the imposition of swirling at the entrance is equivalent to the injection of helicity into a fluid region. The injection is made through the $\mathbf{u}\cdot\boldsymbol{\omega}$-related part in the second term on the right-hand side of Eq. (6), which is rewritten as

$$\int_S \mathbf{n}\cdot\left(-(\mathbf{u}\cdot\boldsymbol{\omega})\mathbf{u}\right)dS \equiv \int_S u_z(\mathbf{u}\cdot\boldsymbol{\omega})dS, \tag{7}$$

at the entrance cross section, where u_z is the axial component of flow.

Here we should stress that $\mathbf{u}\cdot\boldsymbol{\omega}$ is not Galilean-invariant; namely, its magnitude is dependent on the choice of a coordinate system. Throughout the present work, we shall choose the frame fixed to a pipe. In the context of Eq. (7), a swirl motion imposed at the

entrance of a pipe is a source of the helicity of mean flow. In the frame fixed to a pipe, the flow far downstream is reduced to a usual state with no mean-flow helicity.

B. Mean and fluctuation

We use the ensemble averaging $\langle\ \rangle$ and divide a quantity f into the mean and the fluctuation around it, F and f'; namely, we write

$$f = F + f', \quad F = \langle f \rangle, \tag{8}$$

where

$$f = (\mathbf{u}, p, \boldsymbol{\omega}), \quad F = (\mathbf{U}, P, \boldsymbol{\Omega}), \quad f' = (\mathbf{u}', p', \boldsymbol{\omega}'). \tag{9}$$

The mean flow $\mathbf{U}$ obeys

$$\frac{\partial U_i}{\partial t} + \frac{\partial}{\partial x_j} U_i U_j = -\frac{\partial P}{\partial x_i} + \frac{\partial}{\partial x_j}\left(-R_{ij}\right) + \nu \Delta U_i, \tag{10}$$

with the solenoidal condition $\boldsymbol{\nabla} \cdot \mathbf{U} = 0$, where R_{ij} is the Reynolds stress defined by

$$R_{ij} = \langle u_i' u_j' \rangle. \tag{11}$$

From Eq. (3), the vorticity counterpart of Eq. (10) is given by

$$\frac{\partial \boldsymbol{\Omega}}{\partial t} = \boldsymbol{\nabla} \times \left(\mathbf{U} \times \boldsymbol{\Omega} + \mathbf{V}^{(M)}\right) + \nu \Delta \boldsymbol{\Omega}, \tag{12}$$

where the vortex-motive force $\mathbf{V}^{(M)}$ is written as

$$\mathbf{V}^{(M)} = \langle \mathbf{u}' \times \boldsymbol{\omega}' \rangle. \tag{13}$$

The turbulent energy K, which is defined by

$$K = \left\langle \frac{1}{2} \mathbf{u}'^2 \right\rangle, \tag{14}$$

obeys

$$\frac{\partial K}{\partial t} + \boldsymbol{\nabla} \cdot (\mathbf{U} K) = P_K - \varepsilon + \boldsymbol{\nabla} \cdot \mathbf{T}_K, \tag{15}$$

where the production rate P_K, the dissipation rate ε, and the transport rate $\mathbf{T}_K$ are given by

$$P_K = -R_{ij}\frac{\partial U_j}{\partial x_i}, \tag{16}$$

$$\varepsilon = \left\langle \nu\left(\frac{\partial u_j'}{\partial x_i}\right)^2 \right\rangle, \tag{17}$$

$$\mathbf{T}_K = -\left\langle \left(p' + \frac{\mathbf{u}'^2}{2}\right)\mathbf{u}' \right\rangle + \nu\nabla K, \tag{18}$$

respectively.

III. VARIATIONAL APPROACH TO TURBULENCE WITH MEAN-FLOW HELICITY

A. Competition between production and diffusion effects

In Eq. (15), the production rate P_K may become locally negative, but its total amount in a whole fluid region V needs to be positive, that is,

$$\int_V P_K dV > 0, \tag{19}$$

as long as a turbulent state is sustained without the injection of K across a boundary S. We may understand this point by integrating Eq. (15) in V, as

$$\frac{\partial}{\partial t}\int_V K dV = \int_V P_K dV - \int_V \varepsilon dV + \int_S \mathbf{n}\cdot\left(-\mathbf{U}K + \mathbf{T}_K\right)dS, \tag{20}$$

and noting that $\int_V \varepsilon dV$ is nonnegative.

The production rate P_K, which is directly dependent on velocity gradients, expresses the rate of energy drain or energy cascade from mean to fluctuating components of motion. A retarded or reversed velocity profile in a turbulent swirling pipe flow possesses a much steeper velocity gradient in the core region, compared with the nonswirling case. In the sense of energy drain, large P_K resulting from a steep gradient seems to be harmful to the sustainment of such a velocity profile.

The diffusion of fluctuation effects occurs through the last term in Eq. (15). In a steady state, it is reduced to

$$\nabla \cdot \mathbf{T}_K = \varepsilon - P_K + \nabla \cdot (\mathbf{U}K). \tag{21}$$

Apart from the last or advection term, the decrease in positive P_K tends to enhance the importance of $\nabla \cdot \mathbf{T}_K$, that is, the diffusion effect. Strong diffusion effect is also harmful to the sustainment of distinct mean-flow structures. For instance, a dominant diffusion effect is encountered near the centerline region in a nonswirling pipe flow. There we have

$$\nabla \cdot \mathbf{T}_K \cong \varepsilon, \quad P_K \cong 0, \tag{22}$$

and a flattened mean-flow profile occurs. On the other hand, the logarithmic-velocity region with a large mean-velocity gradient is characterized by

$$P_K \cong \varepsilon, \quad \nabla \cdot \mathbf{T}_K \cong 0, \tag{23}$$

leading to a weak-diffusion state.

From these arguments, we may consider that a retarded or reversed velocity profile in a swirling pipe flow is realized under the competition or reconciliation of the production and diffusion effects. The following analysis is based on this concept, and the introduction of helicity is crucial to the realization of a retarded or reversed flow.

B. Derivation of vorticity equation

A retarded or reversed axial velocity in a swirling pipe flow is characterized by the mean velocity gradient, as was noted above. As an indicator of the strength of spatial variation or inhomogeneity of mean velocity in a region V, we introduce

$$\Phi = \int_V \left(\frac{\partial U_j}{\partial x_i} \right)^2 dV. \tag{24}$$

In the light of the energy production or drain rate P_K, the physical meaning of Φ may be interpreted as follows. Under the turbulent-viscosity (ν_T) approximation to the Reynolds stress R_{ij}, P_K is approximated as

$$P_K = \frac{1}{2} \nu_T \left(\frac{\partial U_j}{\partial x_i} + \frac{\partial U_i}{\partial x_j} \right)^2. \tag{25}$$

Equation (25) may be rewritten as

$$P_K = \nu_T \left(\frac{\partial U_j}{\partial x_i} \right)^2 + \nu_T \frac{\partial^2 U_i U_j}{\partial x_i \partial x_j}, \tag{26}$$

using the solenoidal condition $\nabla \cdot \mathbf{U} = 0$. From Eq. (26), we have

$$\int_V P_K dV = \int_V \nu_T \left(\frac{\partial U_j}{\partial x_i} \right)^2 dV + \int_S \nu_T n_i \frac{\partial U_i U_j}{\partial x_j} dS, \tag{27}$$

where the spatial variation of ν_T was neglected. The second term on the right-hand side of Eq. (27) is absorbed into the third term of Eq. (20), and the first term represents the net energy cascade from the mean to fluctuating components of motion. Therefore we may consider that Φ is an indicator of the magnitude of a total amount of P_K, that is, $\int_V P_K dV$.

A mean axial vorticity arising from a mean swirl velocity is an important quantity characterizing a turbulent swirling flow in a pipe. Its combination with a mean axial velocity results in nonvanishing mean-flow helicity. Then as a critical quantity distinguishing between swirling and nonswirling flows, we introduce a total amount of mean-flow helicity, which is defined by

$$\Psi = \int_V \mathbf{U} \cdot \boldsymbol{\Omega} dV. \tag{28}$$

Here we should stress that Φ and Ψ, which are defined by Eqs. (24) and (28), contain no direct effects of the molecular viscosity ν. Therefore the following discussions are relevant to flows at high Reynolds numbers and are not applicable to a near-wall region. Special attention will be paid to global characteristics of a swirling flow in the core region where ν effects are weak.

Effects of helicity on the energy cascade in isotropic turbulence were examined with the aid of the eddy-damped quasi-normal Markovianized (EDQNM) approximation.[14] The study shows that the helicity in the energy-containing range of wavenumber space hampers the cascade of energy towards smaller-scale or higher-wavenumber components of motion. In the light of mean flow, this finding suggests that the existence of helicity in mean flow suppresses the energy cascade to fluctuating parts of motion. With this point in mind, we adopt Ψ as a constraint on Φ and seek the state

$$\Phi = \text{minimum under } \Psi = \text{constant}, \tag{29}$$

by the standard variational method. In mathematical terms, Eq. (29) is given by

$$\delta(\Phi + \lambda\Psi) = 0 \tag{30}$$

with a Lagrange multiplier λ. On applying this variational principle to seek $\mathbf{U}$ leading to the minimum state of Φ, it is necessary to fix $\mathbf{U}$ at the boundary S that surrounds V; namely, we impose

$$\delta\mathbf{U} = 0 \ \text{ at } S. \tag{31}$$

Equation (30) may be evaluated as follows. First, we rewrite Φ as

$$\delta\left(\left(\frac{\partial U_J}{\partial x_i}\right)^2\right) = 2\frac{\partial U_J}{\partial x_i}\frac{\partial}{\partial x_i}\delta U_J = -2\Delta\mathbf{U}\cdot\delta\mathbf{U} + 2\frac{\partial}{\partial x_i}\left(\frac{\partial U_J}{\partial x_i}\delta U_J\right). \tag{32}$$

We substitute Eq. (32) into Eq. (24) and have

$$\delta\Phi = \int_V \left(-2\nu_T\Delta\mathbf{U}\right)\cdot\delta\mathbf{U}dV, \tag{33}$$

since the last part in Eq. (32) vanishes under the constraint (31). Here we should recall that the present method is not applicable to a real solid boundary where molecular effects become dominant. The boundary used in this variational method, S, is not a real solid wall of a pipe and is virtual. Equation (33) may be rewritten as

$$\delta\Phi = \int_V \left(2\nu_T\nabla\times\boldsymbol{\Omega}\right)\cdot\delta\mathbf{U}dV, \tag{34}$$

where use has been made of $\Delta\mathbf{U} = -\nabla\times(\nabla\times\mathbf{U})$.

Similarly, $\delta\Psi$ is calculated as

$$\delta\Psi = \int_V 2\boldsymbol{\Omega}\cdot\delta\mathbf{U}dV - \int_S(\mathbf{n}\times\mathbf{U})\cdot\delta\mathbf{U}dS, \tag{35}$$

giving

$$\delta\Psi = \int_V 2\boldsymbol{\Omega}\cdot\delta\mathbf{U}dV, \tag{36}$$

under Eq. (31).

Equation (30) is combined with Eqs. (34) and (36), leading to

$$\int_V \left(\nabla\times\boldsymbol{\Omega} + \lambda\boldsymbol{\Omega}\right)\cdot\delta\mathbf{U}dV = 0. \tag{37}$$

For arbitrary $\mathbf{U}$, Eq. (37) is satisfied by

$$\mathbf{\Omega} = -\frac{1}{\lambda}\nabla\times\mathbf{\Omega}. \tag{38}$$

In Eq. (38), $\mathbf{\Omega}$ is an axial vector (a vector whose sign does not change under the reflection of coordinates), whereas $\nabla\times\mathbf{\Omega}$ is a polar vector. Then λ needs to be a pseudo-scalar (a scalar whose sign changes under the reflection). Concerning λ, we shall discuss the following points:

(a) The magnitude of λ is related to the distance from the centerline axis to the local-maximum point of mean velocity (see Sec. IVB);

(b) The sign of λ is linked with that of Ψ (a total amount of helicity) (see Appendix);

(c) In the light of turbulence modeling, λ is related to the turbulence helicity $\langle\mathbf{u}'\cdot\boldsymbol{\omega}'\rangle$ (see Sec. IVE).

We integrate Eq. (38), and have

$$\mathbf{U} = -\frac{1}{\lambda}\mathbf{\Omega} + \nabla\phi, \tag{39}$$

where ϕ is an arbitrary scalar function. Here we should stress the following two points. First, the essence of Eq. (38) manifests itself in Eq. (39). The first term on the right-hand side signifies that the mean velocity and vorticity are aligned with each other, leading to nonvanishing mean-flow helicity, as is consistent with the requirement for nonvanishing Ψ in Eq. (30). Second, the mean velocity may be expressed in a simple form, with the aid of the mean vorticity. By taking the curl of Eq. (38) , we have

$$\left(\Delta + \lambda^2\right)\mathbf{\Omega} = 0. \tag{40}$$

With the aid of a solution of Eq. (40), we may examine properties of the mean motion in the presence of helicity effects. This point will become clear in later discussions.

IV. ANALYSIS OF A SWIRLING PIPE FLOW

A. Solution of vorticity equation in cylindrical geometry

We adopt the cylindrical coordinates (r,θ,z), and z is along the central axis of the cylinder. The velocity $\mathbf{U}$ is written as

$$\mathbf{U} = \left(0, U_\theta(r), U_z(r)\right). \tag{41}$$

Here we should remark on the variation of $\mathbf{U}$ along the z axis. In the case of a swirling pipe flow, this variation is very important in relation to the relaxation of a retarded or reversed axial flow to a usual pipe flow. In the present variational approach, this relaxation is dealt with through the implicit change of the parameter λ. The increase in λ corresponds to the decrease in the swirling effect. This point will become clear in later discussions.

The mean vorticity $\mathbf{\Omega}$, whose component is given by

$$\mathbf{\Omega} = \left(0, \Omega_\theta(r), \Omega_z(r)\right), \tag{42}$$

is written in terms of $\mathbf{U}$ as

$$\Omega_\theta = -\frac{dU_z}{dr}, \tag{43}$$

$$\Omega_z = \frac{1}{r}\frac{d}{dr}\left(rU_\theta\right). \tag{44}$$

From Eq. (39), $\mathbf{U}$ is related to $\mathbf{\Omega}$ as

$$U_\theta = -\frac{1}{\lambda}\Omega_\theta + \frac{\partial \phi}{r\partial \theta}, \tag{45}$$

$$U_z = -\frac{1}{\lambda}\Omega_z + \frac{\partial \phi}{\partial z}. \tag{46}$$

Moreover, we have the relation

$$\Omega_\theta = \frac{1}{\lambda}\frac{d\Omega_z}{dr}, \tag{47}$$

from Eq. (38).

Apart from a scalar function ϕ, Eqs. (45) - (47) show that $\mathbf{U}$ may be expressed using the axial vorticity component Ω_z; namely, Ω_z plays a critical role in a swirling flow. The z component of Eq. (40) is

$$\frac{d^2\Omega_z}{dr^2} + \frac{1}{r}\frac{d\Omega_z}{dr} + \lambda^2\Omega_z = 0. \tag{48}$$

The solution of Eq. (48), which is regular at the centerline ($r = 0$), is given by

$$\Omega_z = \Omega_z^{(C)} J_0(\lambda r), \tag{49}$$

where J_n is the first-order Bessel function of the nth order, and

$$\Omega_z^{(C)} = \Omega_z(0). \tag{50}$$

From Eqs. (47) and (49), we have

$$\Omega_\theta = -\Omega_z^{(C)} J_1(\lambda r). \tag{51}$$

Through the combination of Eqs. (45) and (46) with Eqs. (49) and (51), $\mathbf{U}$ has been expressed in terms of the Bessel function J_n.

The profiles of J_0 and J_1 are shown in Fig. 1, and their first two zero's, that is, $x_m^{(n)}$ obeying $J_n\left(x_m^{(n)}\right) = 0$ $(m = 1, 2)$, are given by

$$x_1^{(0)} = 2.4, \quad x_2^{(0)} = 5.5, \tag{52}$$

$$x_1^{(1)} = 3.8, \quad x_2^{(1)} = 7.0, \tag{53}$$

respectively.

B. Estimate of retarded or reversed centerline velocity

A retarded axial flow U_z in a pipe is depicted schematically in Fig. 2 (a), with the tangential velocity U_θ in Fig. 2 (b) (a is the radius of the pipe). From Eq. (43), the maximum-velocity point of U_z, r_M, corresponds to the zero point of Ω_θ, as is schematically shown in Fig. 2 (c); namely, we have

$$\Omega_\theta(r_M) = 0 \tag{54a}$$

or

$$J_1(\lambda r_M) = 0 \tag{54b}$$

from Eq. (51). The first zero in Eq. (53) gives

$$|\lambda| r_M = 3.8. \tag{55}$$

Here we should note that λ may take both signs. The sign of λ is dependent on that of a total amount of helicity in the region $r \le r_M$, as is shown in Appendix. We first choose positive λ and refer to negative λ later.

From $r_M \le a$, we have

$$\lambda \ge \frac{3.8}{a}. \tag{56}$$

With λ increasing from $3.8/a$, r_M approaches to the central axis, and the negative region of Ω_θ between the central axis and r_M shrinks. In the context of Eq. (30), $\lambda \to \infty$ signifies $\Psi \to 0$, that is, vanishing global or mean-flow helicity. As a result, Eq. (46) is reduced to the usual axial velocity in a nonswirling pipe flow; namely, we have

$$U_z \to U^{(N)} \quad \text{as} \quad \lambda \to \infty. \tag{57}$$

Here $U^{(N)}$ denotes the axial velocity of a pipe flow in the limit of large Reynolds number and is uniform across the cross section, except the near-wall region. Equation (57) corresponds to the choice

$$\phi = U^{(N)} z + \phi_0, \tag{58}$$

with a constant ϕ_0, resulting in

$$U_z = U^{(N)} - \frac{1}{\lambda}\Omega_z, \tag{59}$$

$$U_\theta = -\frac{1}{\lambda}\Omega_\theta, \tag{60}$$

for finite λ [we should note that Eq. (60) satisfies the symmetry condition at the centerline, namely, $U_\theta(0) = 0$].

The present variational method is not proper for the weak-helicity or large-λ case that results in no constraint. This point may be seen in relation to the second zero of J_1 [the latter of Eq. (53)]; namely, we have

$$\Omega_\theta(r) \le 0 \quad (\lambda r \ge 7.0). \tag{61}$$

In an actual flow, Ω_θ should be always positive for $r > r_M$, owing to the noslip boundary condition at the wall. In the present variational method, no molecular-viscosity

effect dominant near the wall is taken into account. This fact indicates that the present solution should be applied to the region off the wall, that is,

$$r \le r_M, \tag{62}$$

which is related to the first zero of J_1. In what follows, we shall focus attention on the centerline velocity, which is a primary interest of this work.

On the centerline ($r = 0$), Eq. (59) is given by

$$U_C^{(S)} \equiv U_z(0) = U^{(N)} - \frac{\Omega_z^{(C)}}{\lambda}, \tag{63}$$

which is written as

$$\frac{U_C^{(S)}}{U^{(N)}} = 1 - \frac{\Omega_z^{(C)}}{\lambda U^{(N)}}, \tag{64}$$

in nondimensional form. We use Eq. (55) for positive λ and express Eq. (64) as

$$\frac{U_C^{(S)}}{U^{(N)}} = 1 - 0.26\frac{r_M \Omega_z^{(C)}}{U^{(N)}}, \tag{65}$$

in terms of measurable quantities.

The tangential velocity U_θ is expressed as

$$U_\theta = \frac{\Omega_z^{(C)}}{\lambda} J_1(\lambda r), \tag{66}$$

from Eqs. (51) and (60). Near the centerline, U_θ is approximated as

$$U_\theta \cong W_C(r) \equiv \frac{\Omega_z^{(C)}}{2} r. \tag{67}$$

We use Eq. (67) and eliminate $\Omega_z^{(C)}$ from Eq. (65). Then we have

$$\frac{U_C^{(S)}}{U^{(N)}} = 1 - \alpha^{(V)} \frac{W_C(r)}{r} \frac{r_M}{U^{(N)}}, \tag{68}$$

where $\alpha^{(V)}$ is the proportional constant theoretically obtained from the variational method and is given by

$$\alpha^{(V)} = 0.53. \tag{69}$$

In the use of Eq. (68), we should note that r is located near the centerline. In the later comparison with observations, we adopt $r = 0.2a$.

The second term on the right-hand side of Eq. (65) represents the degree of retardation or reversal of an axial velocity on the center line. It is proportional to the mean vorticity near the axis, $\Omega_z^{(C)}$, which is related to the swirl velocity $W_C(r)$, as in Eq. (68). It is also proportional to r_M (the point of maximum axial velocity). The observation indicates that increasing $\Omega_z^{(C)}$ leads to larger r_M, resulting in the larger retardation of the centerline velocity or its reversal. This tendency is consistent with Eq. (65) or (68).

From the foregoing findings, we may conclude that the retardation or reversal of the centerline velocity is tightly linked with positive $\Omega_z^{(C)}$. In the above discussion, we chose positive λ. In the case of negative λ, Ω_θ becomes positive for $r < r_M$ from Eq. (51) for positive $\Omega_z^{(C)}$. From Eq. (43), such Ω_θ arises from a retarded axial flow pointing to the negative z direction, while keeping the same tangential velocity U_θ [note that U_θ is unchanged under the change of the sign of λ from Eq. (66) since $J_1(\lambda r)/\lambda$ is an even function of λ].

C. Comparison with observations

Let us compare a theoretically-derived expression of the centerline velocity, Eq. (68), with the observation by Kitoh.[1] For this purpose, we write

$$\frac{U_C^{(S)}}{U^{(N)}} = \chi^{(S)}(\alpha), \tag{70}$$

with

$$\chi^{(S)}(\alpha) = 1 - \alpha \frac{W_C(r)}{r} \frac{r_M}{U^{(N)}}. \tag{71}$$

An accurate measurement of a strongly swirling flow with a reversed flow is difficult, specifically, near the centerline, owing to the highly helical motion and its related fluctuations. In reality, the swirl velocity U_θ does not vanish exactly in the observation by Kitoh. In the present use of the observational data, we extrapolated them from the off-centerline region, and estimated $U_C^{(S)}/U^{(N)}$, which is given as $\chi_{obsev}^{(S)}$ in Table 1. Here we should emphasize that $U^{(N)}$ is approximated by the observed centerline velocity in the absence of a swirling. In Kitoh's work,[1] the Reynolds number (R),

which is defined using a and U_B (the bulk velocity, that is, the mean velocity across the cross section), is 50000 - 80000. The centerline velocity is proper to the estimate of $U^{(N)}$ since the region is subject to least effects of molecular viscosity.

We adopted three cases with reversed centerline velocity, from Kitoh's observation at $R = 50000$. As was noted above, the data in the close vicinity of the centerline rather scatter. Then we use the swirl velocity at $r = 0.2a$ for the estimate of $\Omega_z^{(C)}$. In the observation, the data are nondimensionalized using U_B, which is related to $U^{(N)}$ as $U^{(N)} = 1.1U_B$.

As may be seen from Table 1, the theoretical results with $\alpha = \alpha^{(V)}$ $(= 0.53)$ are consistent with the tendency of the observed reversed centerline velocity, but the magnitude of reversal is overestimated. We reduce the numerical coefficient in Eq. (68), α, from $\alpha^{(V)}$ to about its half, $\alpha = 0.3$. The estimate based on this alternation is also given in Table 1, and is in fair agreement with the observation. This fact suggests that the vorticity equation (38) captures parts of the important features of a swirling pipe flow.

From the engineering viewpoint, it is important to estimate the degree of axial-velocity retardation or reversal in close relation to flows inside engines. In the present work, the retardation or reversal of the centerline velocity has been shown to be linked with the centerline axial vorticity $\Omega_z^{(C)}$ and the maximum-velocity location r_M. If an empirical expression for r_M, such as

$$\frac{r_M}{a} = f\left(\Omega_z^{(C)}, R\right) \tag{72}$$

could be obtained from observations or otherwise, Eq. (71) would be useful for the estimate of flow reversal ($\Omega_z^{(C)}$ needs to be nondimensionalized properly).

D. Interpretation of a laminarlike axial velocity in an axially rotating pipe

We may mention a turbulent flow in an axially rotating pipe as an interesting instance of pipe flows whose mean-flow behavior is entirely different from the foregoing swirling pipe flow. In this flow, the rotation of a pipe, which is imposed on the usual pressure-driven flow, gives rise to the change from a flattened velocity profile to an elongated or laminarlike profile. The axial and swirl components of mean velocity, U_z and U_θ, are depicted schematically in Figs. 3 (a) and (b), respectively. The elongation of U_z is enhanced with the increasing rotation number

$$N = \frac{a\omega_P}{U_B}, \tag{73}$$

where ω_P is the angular velocity of a pipe. The tangential velocity U_θ is retarded, compared with the solid-rotation velocity $r\omega_P$.

A flow in an axially rotating pipe has been examined intensively by observations,[15-17] direct numerical simulation,[18,19] and third-order explicit algebraic[6-8] and second-order[20,21] turbulence models. Specifically, this flow is a proper benchmark case for testing newly proposed turbulence models since Coriolis- and centrifugal-force effects included in the flow are generally difficult to treat properly by those models. In the explicit algebraic models,[6-8] the elongation of an axial velocity profile may be explained through the terms in the Reynolds stress R_{ij} that are of the third order in mean velocity-strain and vorticity tensors. On the other hand, in the second-order modeling, the axial shear stress R_{rz}, which determines the behavior of an axial velocity, is affected by the swirl velocity through the swirl shear stress $R_{r\theta}$,[21] causing the elongation.

Let us see the elongation of an axial velocity profile from a viewpoint of the present variational approach. Here we should emphasize that the following discussion is not to aim at explaining this elongation mechanism in a quantitative manner, but at abstracting a quantity that is closely associated with the mechanism.

Helicity is a frame-dependent quantity, and the frame fixed to a pipe was adopted in the analysis of a swirling pipe flow. In a rotating pipe flow, fluid is driven by pipe rotation through viscous effects. Those effects, however, are not taken into account in the present variational method. In the following discussion, we also adopt the frame fixed to a pipe, that is, the frame rotating with ω_P. This choice of frame is helpful for partially incorporating effects of pipe rotation.

In the rotating frame, we make use of the finding obtained in Sec IV, especially, Eqs. (64) and (66). After Eq. (64), we write the centerline velocity of a rotating pipe flow, $U_C^{(R)}$, as

$$\frac{U_C^{(R)}}{U^{(N)}} = 1 - \frac{\Omega_z^{(C)}}{\lambda U^{(N)}}, \tag{74}$$

which shows that the sign of the centerline vorticity has a large influence on the centerline velocity.

Under U_z depicted in Fig. 3 (a), Ω_θ is positive from Eq. (43). Observations of an axially rotating pipe flows[15,16] show that fluid rotates with the angular velocity slower than ω_P, as is depicted schematically in Fig. 3 (b). Then U_θ is negative in the rotating frame [Fig. 3 (c)], and λ is positive from Eq. (60). As a result, we have

$$\Omega_z^{(C)} < 0, \tag{75}$$

from Eq. (51). Negative $\Omega_z^{(C)}$ makes a sharp contrast with the case of a swirling pipe flow in Sec. IVC. In the latter, positive $\Omega_z^{(C)}$ was shown to be critical for the retardation or reversal of the centerline velocity. From Eqs. (74) and (75), we have

$$\frac{U_C^{(R)}}{U^{(N)}} > 1; \tag{76}$$

namely, the velocity near the centerline is elongated, compared with the non-rotating case.

E. Towards turbulence modeling

In the present variational approach, we have some important points to be completed. One of them is the incorporation of the present finding into turbulence modeling. This point is also associated with the specification of a pseudoscalar λ that occurs in Eq. (38) etc. In general, helicity is not a Galilean-invariant quantity, as has already been noted, whereas the vorticity equation (38) must be Galilean-invariant. Then λ needs to be related to a Galilean-invariant pseudoscalar. A representative Galilean-invariant pseudoscalar is the turbulent helicity H, which is defined by

$$H = \langle \mathbf{u}' \cdot \boldsymbol{\omega}' \rangle. \tag{77}$$

A total amount of helicity, Ψ, is conserved so long as there are no molecular-viscosity effect and no helicity flux across a boundary. This property is very important in close relation to turbulence modeling. The turbulent helicity H obeys the equation whose mathematical structure is clear and quite similar to Eq. (15).[12,13] It is written as

$$\frac{\partial H}{\partial t} + \nabla \cdot (\mathbf{U} H) = P_H - \varepsilon_H + \nabla \cdot \mathbf{T}_H, \tag{78}$$

where three terms on the right-hand side correspond to those in Eq. (15), respectively, which are defined by

$$P_H = \frac{\partial R_{ij}}{\partial x_j}\Omega_i - R_{ij}\frac{\partial \Omega_i}{\partial x_j}, \tag{79}$$

$$\varepsilon_H = 2\nu\left\langle \frac{\partial u_j'}{\partial x_i}\frac{\partial \omega_j'}{\partial x_i}\right\rangle, \tag{80}$$

$$\mathbf{T}_H = -\left\langle (\mathbf{u}'\cdot\boldsymbol{\omega}')\mathbf{u}'\right\rangle + \left\langle \left(\frac{1}{2}\mathbf{u}'^2 - p'\right)\boldsymbol{\omega}'\right\rangle + \nu\nabla H. \tag{81}$$

In a previous work,[12] we analyzed effects of H on R_{ij} with the aid of a two-scale direct-interaction approximation (TSDIA) and obtained

$$R_{ij} = \frac{2}{3}K\delta_{ij} - C_v\frac{K^2}{\varepsilon}S_{ij} + C_H\left[\Omega_i\frac{\partial}{\partial x_j}\left(\frac{K^4}{\varepsilon^3}H\right) + \Omega_j\frac{\partial}{\partial x_i}\left(\frac{K^4}{\varepsilon^3}H\right)\right]_D, \tag{82}$$

where C_v and C_H are model constants, and

$$S_{ij} = \frac{\partial U_j}{\partial x_i} + \frac{\partial U_i}{\partial x_j}, \tag{83}$$

$$\left[A_{ij}\right]_D = A_{ij} - \frac{1}{3}A_{\ell\ell}\delta_{ij}. \tag{84}$$

This model combined with Eq. (78) was applied to the case of weak entrance swirl intensity in a swirling pipe flow and was confirmed to reproduce retardation of an axial velocity. The helicity effect expressed by the third term in Eq. (82), however, was not strong enough to explain the strong-swirl case.

In the light of Eq. (12), a stationary state at a high Reynolds number may arise from the condition

$$\mathbf{U}\times\boldsymbol{\Omega} + \mathbf{V}^{(M)} = 0. \tag{85}$$

From Eqs. (39) and (85), we have

$$\mathbf{V}^{(M)} = -\nabla\phi\times\boldsymbol{\Omega}. \tag{86a}$$

We substitute Eq. (38) into Eq. (86a) and write

$$\mathbf{V}^{(M)} = \nabla\chi\times(\nabla\times\boldsymbol{\Omega}) = -\nabla\chi\times\Delta\mathbf{U}, \tag{86b}$$

where a pseudoscalar χ is defined by

$$\chi = \frac{\phi}{\lambda}. \tag{87}$$

The i component of Eq. (86b) is rewritten in the form

$$V_i^{(M)} = -\varepsilon_{i\ell m}\frac{\partial \chi}{\partial x_\ell}\frac{\partial^2 U_m}{\partial x_j^{\,2}} = \frac{\partial}{\partial x_j}\left(-\varepsilon_{i\ell m}\frac{\partial \chi}{\partial x_\ell}\frac{\partial U_m}{\partial x_j}\right) + \varepsilon_{i\ell m}\frac{\partial^2 \chi}{\partial x_j \partial x_\ell}\frac{\partial U_m}{\partial x_j}, \tag{88}$$

where $\varepsilon_{ij\ell}$ is the alternating tensor. We pay special attention to the first term in the second relation of Eq. (88). Noting that $\mathbf{V}^{(M)}$ corresponds to the divergence of R_{ij}, we model the contribution of the first term to R_{ij} as

$$\left[\varepsilon_{i\ell m}\frac{\partial U_m}{\partial x_j}\frac{\partial \chi}{\partial x_\ell} + \varepsilon_{j\ell m}\frac{\partial U_m}{\partial x_i}\frac{\partial \chi}{\partial x_\ell}\right]_D. \tag{89}$$

From the viewpoint of turbulence modeling, it is sufficient to model a pseudoscalar χ, not each of ϕ and λ. From dimensional analysis, we write

$$\chi = C_V \frac{K^4}{\varepsilon^3} H, \tag{90}$$

with a constant C_V. Equation (90) corresponds to the choice of λ that is proportional to the inverse of H. This modeling is consistent with the fact that large $|\lambda|$ corresponds to a weak-helicity case.

Equation (89) is rewritten as

$$\frac{1}{2}\left[\varepsilon_{i\ell m}S_{jm}\frac{\partial \chi}{\partial x_\ell} + \varepsilon_{j\ell m}S_{im}\frac{\partial \chi}{\partial x_\ell}\right]_D + \frac{1}{2}\left[\varepsilon_{i\ell m}\Omega_{jm}\frac{\partial \chi}{\partial x_\ell} + \varepsilon_{j\ell m}\Omega_{im}\frac{\partial \chi}{\partial x_\ell}\right]_D. \tag{91}$$

Here Ω_{ij} is the mean vorticity tensor defined by

$$\Omega_{ij} = \frac{\partial U_j}{\partial x_i} - \frac{\partial U_i}{\partial x_j}, \tag{92a}$$

which is related to $\mathbf{\Omega}$ as

$$\Omega_{ij} = \varepsilon_{ij\ell}\Omega_\ell. \tag{92b}$$

We substitute Eq. (92b) into the second or Ω_{ij}-related term in Eq. (91) and have

$$\frac{1}{2}\left[\Omega_i \frac{\partial \chi}{\partial x_j} + \Omega_j \frac{\partial \chi}{\partial x_i}\right]_D \tag{93}$$

(note $\varepsilon_{ij\ell}\varepsilon_{imn} = \delta_{im}\delta_{jn} - \delta_{in}\delta_{jm}$). Expression (93) with Eq. (90) coincides with the third term in Eq. (82) that was derived on the basis of the TSDIA. On the other hand, the first term in Eq. (91) is missing in the TSDIA model. Specifically, the fact that this new H effect occurs through the combination with S_{ij} is interesting since the S_{ij} effect in Eq. (82) only contributes to the destruction of distinct mean-flow structures.

We replace the third term in Eq. (82) with Eq. (89) as

$$R_{ij} = \frac{2}{3}K\delta_{ij} - C_\nu \frac{K^2}{\varepsilon} S_{ij} + \left[\varepsilon_{i\ell m}\frac{\partial U_m}{\partial x_j}\frac{\partial \chi}{\partial x_\ell} + \varepsilon_{j\ell m}\frac{\partial U_m}{\partial x_i}\frac{\partial \chi}{\partial x_\ell}\right]_D, \tag{94a}$$

or

$$R_{ij} = \frac{2}{3}K\delta_{ij} - C_\nu \frac{K^2}{\varepsilon} S_{ij} + C_S\left[\varepsilon_{i\ell m}S_{jm}\frac{\partial \chi}{\partial x_\ell} + \varepsilon_{j\ell m}S_{im}\frac{\partial \chi}{\partial x_\ell}\right]_D$$

$$+\left[\varepsilon_{i\ell m}\Omega_{jm}\frac{\partial \chi}{\partial x_\ell} + \varepsilon_{j\ell m}\Omega_{im}\frac{\partial \chi}{\partial x_\ell}\right]_D \tag{94b}$$

as a more general expression (the numerical factor $1/2$ is not essential and may be absorbed into χ). Here Eq. (94b) with $C_S = 1$ is reduced to Eq. (94a). Through this procedure, we can include a new helicity effect on R_{ij}, while keeping the previous one that has already been confirmed to contribute to the retardation of a mean axial flow. The test of Eq. (94a) or (94b) is left for future work.

V. CONCLUDING REMARKS

In this work, we formulated a variational approach to a turbulent flow with the helicity arising from a global rotational motion of fluid. A solution of the resulting vorticity equation was sought in cylindrical geometry and was applied to the discussion about a swirling pipe flow. Specifically, we estimated the reversed central-axis velocity and made the comparison with observations. As a result, the qualitative feature of the observed reversed velocity was reproduced. We also interpreted a laminarlike velocity profile occurring in an axially rotating pipe, with the aid of the same solution. In both of

flows, the centerline vorticity was shown to have a large influence on the centerline velocity. Through these findings, the concept of helicity was confirmed to be useful in understanding of a coexistence mechanism of turbulent production and diffusion effects in swirling flows. Moreover we also referred to helicity effects on the Reynolds stress in the light of turbulence modeling.

ACKNOWLEDGMENTS

The authors (A. Y., N. Y., and S. N.) are grateful to Dr Fujihiro Hamba for the discussion about helicity effects on the Reynolds stress. The authors are also grateful to the referees for the improvement of the presentation of the manuscript. This work is partly supported by the Grant-in-Aid for Scientific Research of Ministry of Education, Culture, Sports, Science and Technology Japan, by the collaboration programme of National Institute for Fusion Science and by the collaboration programme of the Research Institute for Applied Mechanics of Kyushu University.

APPENDIX: EFFECTS OF NONAXISYMMETRIC MOTION

In Sec. IV, we focused attention on the axisymmetric component of flow. This approach is natural from the standpoint of examining the relationship with an ensemble-mean state of flow. In order to relax the axisymmetric condition, we write

$$\mathbf{U} = \left(U_r(r,\theta), U_\theta(r,\theta), U_z(r,\theta)\right), \tag{A1}$$

$$\boldsymbol{\Omega} = \left(\Omega_r(r,\theta), \Omega_\theta(r,\theta), \Omega_z(r,\theta)\right). \tag{A2}$$

From the vorticity equation (38), we have

$$\Omega_r = -\frac{1}{\lambda}\frac{\partial \Omega_z}{r\partial\theta}. \tag{A3}$$

Under the nonaxisymmetric condition, the z component of Eq. (40) is written as

$$\frac{\partial^2 \Omega_z}{\partial r^2} + \frac{1}{r}\frac{\partial \Omega_z}{\partial r} + \frac{1}{r^2}\frac{\partial^2 \Omega_z}{\partial \theta^2} + \lambda^2 \Omega_z = 0. \tag{A4}$$

A general solution of Eq. (A4) is given by

$$\Omega_z = \Omega_z^{(C)} J_0(\lambda r) + \sum_{n=1}^{\infty}\left(\Omega_{zn}^{(c)} \cos n\theta + \Omega_{zn}^{(s)} \sin n\theta\right) J_n(\lambda r), \tag{A5}$$

where $\Omega_{zn}^{(c)}$ and $\Omega_{zn}^{(s)}$ are numerical coefficients. From Eqs. (47) and (A3), we have

$$\Omega_\theta = -\Omega_z^{(C)} J_1(\lambda r) + \frac{1}{\lambda}\sum_{n=1}^{\infty}\left(\Omega_{zn}^{(c)} \cos n\theta + \Omega_{zn}^{(s)} \sin n\theta\right)\frac{d}{dr} J_n(\lambda r), \tag{A6}$$

$$\Omega_r = \frac{1}{\lambda}\sum_{n=1}^{\infty}\left(n\Omega_{zn}^{(c)} \sin n\theta - n\Omega_{zn}^{(s)} \cos n\theta\right)\frac{J_n(\lambda r)}{r}. \tag{A7}$$

From Eqs. (39) and (A5) - (A7), $\mathbf{U}$ may be expressed as

$$U_z = U^{(N)} - \frac{1}{\lambda}\left(\Omega_z^{(C)} J_0(\lambda r) + \sum_{n=1}^{\infty}\left(\Omega_{zn}^{(c)} \cos n\theta + \Omega_{zn}^{(s)} \sin n\theta\right) J_n(\lambda r)\right), \tag{A8}$$

$$U_\theta = \frac{\Omega_z^{(C)}}{\lambda} J_1(\lambda r) - \frac{1}{\lambda^2}\sum_{n=1}^{\infty}\left(\Omega_{zn}^{(c)} \cos n\theta + \Omega_{zn}^{(s)} \sin n\theta\right)\frac{d}{dr} J_n(\lambda r), \tag{A9}$$

$$U_r = -\frac{1}{\lambda^2}\sum_{n=1}^{\infty}\left(n\Omega_{zn}^{(c)} \sin n\theta - n\Omega_{zn}^{(s)} \cos n\theta\right)\frac{J_n(\lambda r)}{r}. \tag{A10}$$

In order to simply see effects of nonaxisymmetric components, we retain the lowest-order component as

$$\Omega_{zn}^{(c)} = \Omega_{z1}^{(c)}\delta_{n1},\ \Omega_{zn}^{(s)} = 0. \tag{A11}$$

The present solution is not valid in the near-wall region, as is noted in the main text. In the calculation of Φ [Eq. (24)] and Ψ [Eq. (28)], we limit the volume integral to the range $r \le r_M$ per unit length of a cylinder; namely, we write

$$\int_V dV = \int_0^{r_M} dr \int_0^{2\pi} r d\theta. \tag{A12}$$

After a lengthy mathematical manipulation, we have

$$\Phi = 2\pi\Omega_z^{(C)2}(\lambda r_M)^2 J_0(\lambda r_M)^2 + \pi\Omega_{z1}^{(c)2}\left((\lambda r_M)^2 J_0(\lambda r_M)^2 + 2\left(1 - J_0(\lambda r_M)^2\right)\right), \tag{A13}$$

and

$$\Psi = \frac{\pi r_M^{\ 2}}{\lambda}\left(2\Omega_z^{(C)2} + \Omega_{z1}^{(c)2}\right), \tag{A14}$$

where use has been made of Eq. (54b). Equation (A14) shows the relation between the eigenvalue λ and the helicity of mean flow, Ψ. We can confirm that the sign of λ is related to that of Ψ. By use of Eq. (A14), Φ is rewritten as

$$\Phi = J_0(\lambda r_M)^2 \lambda^3 \Psi + 2\pi\Omega_{z1}^{(c)2}\left(1 - J_0(\lambda r_M)^2\right). \tag{A15}$$

From Eq. (55), we have

$$J_0(\lambda r_M) = -0.36. \tag{A16}$$

In Eq. (A15), the second term is positive from Eq. (A16). This fact indicates that the minimum-Φ state under the constraint of fixed Ψ is realized for

$$\Omega_{z1}^{(c)} = 0. \tag{A17}$$

This result is consistent with Eq. (29) seeking the minimum state of Φ under the axisymmetric condition.

REFERENCES

[1]O. Kitoh, "Experimental study of turbulent swirling flow in a straight pipe," J. Fluid Mech. **225**, 445 (1991).

[2]T. Kobayashi and M. Yoda, "Modified $K-\varepsilon$ model for turbulent swirling flow in a straight pipe," JSME Intl. J. **30**, 66 (1987).

[3]D. B. Taulbee. "An improved algebraic Reynolds stress model and corresponding nonlinear stress model," Phys. Fluids A **4**, 2555 (1992).

[4]T. Gatski and C. G. Speziale, "On explicit algebraic stress models for complex turbulent flows." J. Fluid Mech. **254**, 59 (1993).

[5]K. Abe, T. Kondoh, and Y. Nagano, "On Reynolds-stress expressions and near-wall scaling parameters for predicting wall and homogeneous turbulent shear flows," Intl. J. Heat and Fluid Flow **18**, 266 (1997).

[6]T. J. Craft, B. E. Launder, and K. Suga, "Prediction of turbulent transitional phenomena with a nonlinear eddy-viscosity model," Intl. J. Heat and Fluid Flow **18**, 15 (1997).

[7]T. -H. Shih, J. Zhu, W. Liou, K. -H. Chen, N. -S. Liu, and J. L. Lumley, "Modeling of turbulent swirling flows," NASA TM 113112 (1997).

[8]S. Wallin and A. V. Johansson, "An explicit algebraic Reynolds stress model for incompressible and compressible turbulent flows," J. Fluid Mech. **403**, 89 (2000).

[9]C. G. Speziale, S. Sarkar, and T. B. Gatski, "Modelling the pressure-strain correlation of turbulence: An invariant dynamical systems approach," J. Fluid Mech. **227**, 245 (1991).

[10]N. Shima, "Prediction of turbulent boundary layers with a second-moment closure: Part 1 — Effects of periodic pressure gradient, wall transpiration, and free-stream turbulence," J. Fluids Eng. **56**, 115 (1993).

[11]J. C. Chen and C. A. Lin, "Computations of strongly swirling flows with quadratic pressure-strain model," in *11th Symp. Turbulent Shear Flows* (Institut National Polytechnique, Unversité Joseph Fourier, Grenoble, 1997), p. 3-59.

[12]N. Yokoi and A. Yoshizawa, " Statistical analysis of the effects of helicity in inhomogeneous turbulence," Phys. Fluids A 5, **464** (1993).

[13]A. Yoshizawa, *Hydrodynamic and Magnetohydrodynamic Turbulent Flows: Modelling and Statistical Theory* (Kluwer, Dordrecht, 1998).

[14]J. C. André and M. Lesieur. "Influence of helicity on the evolution of isotropic turbulence at high Reynolds number," J. Fluid Mech. **81**, 187 (1977).

[15]K. Kikuyama, M. Murakami, K. Nishibori, and K. Maeda, "Flow in an axially rotating pipe (a calculation of flow in the saturated region)," Bull. JSME 26, 506 (1983).

[16]G. Reich and H. Beer, "Fluid flow and heat transfer in axially rotating pipe 1. Effect of rotation on turbulent pipe flow, Intl. J. Heat Mass Transfer **32**, 551 (1989).

[17]S. Imao, M. Itoh and T. Harada, "Turbulent characteristics of the flow in an axially rotating pipe," Intl. J. Heat Fluid Flow, **17**, 444 (1996).

[18]P. Orlandi, "Helicity fluctuations and turbulent energy production in rotating and non-rotating pipes," Phys. Fluids **9**, 2045 (1997).

[19]P. Orlandi and M. Fatica, "Direct simulations of turbulent flow in a pipe rotating about its axis, " J. Fluid Mech. **343**, 43 (1997).

[20]B. A. Pettersson, H. I. Andersson, and A. S. Brunvoll, "Modeling near-wall effects in axially rotating pipe flow by elliptic relaxation," AIAA J. **36**, 1164 (1998).

[21]C. G. Speziale, B. A. Younis, and S. A. Berger, "Analysis and modelling of turbulent flow in an axially rotating pipe," J. Fluid Mech. **407**, 1 (2000).

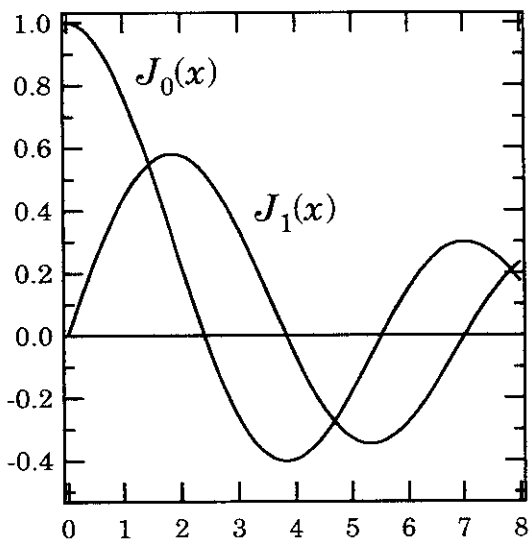

Fig. 1. Bessel function $J_n(x)$ $(n = 0, 1)$.

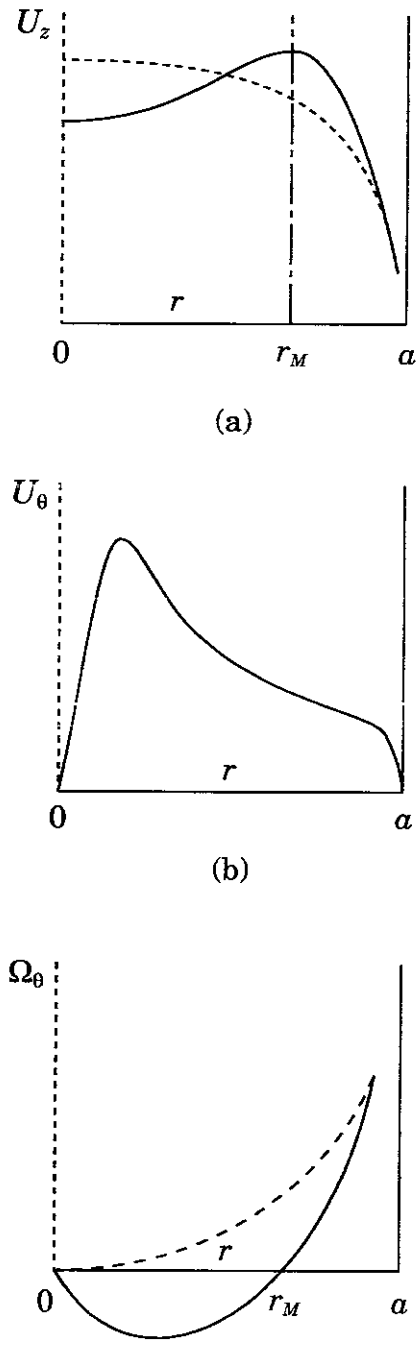

Fig. 2. Swirling flow in a pipe. (a) Mean axial velocity U_z (the dashed line represents the case of no swirling); (b) Mean tangential velocity U_θ ; (c) Mean tangential vorticity Ω_θ.

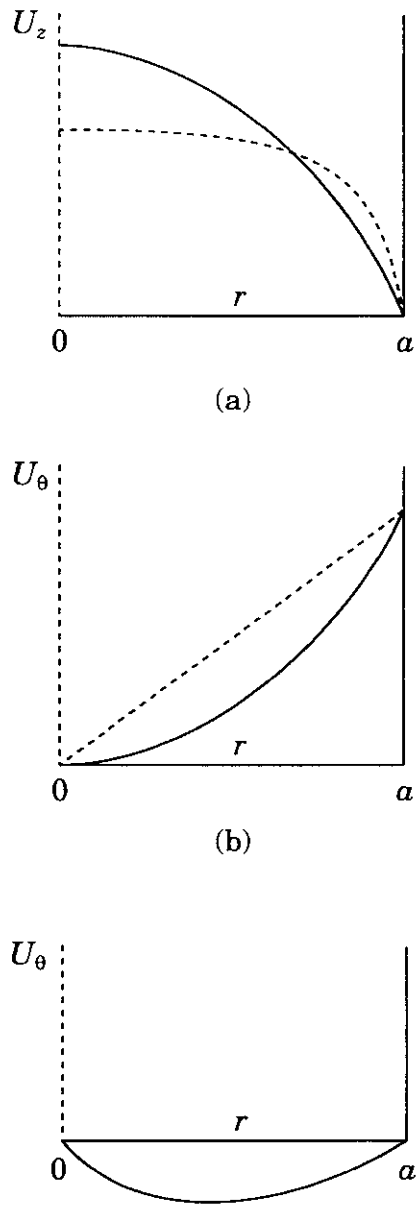

Fig. 3. Rotating pipe flow. (a) Mean axial velocity U_z (the dashed line represents the case of no rotation); (b) Mean tangential velocity U_θ ; (c) Mean tangential velocity U_θ in the frame fixed to a pipe.

Table 1. Comparison with the observed rate of the reversed central-axis velocity ($\lambda a = 3.8a / r_M$).

	$W_C(0.2a)/U^{(N)}$	r_M / a	λa	$\chi^{(S)}_{obsev}$	$\chi^{(S)}(\alpha^{(V)})$	$\chi^{(S)}(0.3)$
Case A	1.7	0.86	4.4	- 0.88	- 2.8	- 1.2
Case B	1.4	0.85	4.4	- 0.76	- 2.1	- 0.80
Case C	1.4	0.79	4.8	- 0.59	- 1.9	- 0.62

Recent Issues of NIFS Series

NIFS-660 T Watari, T Mutoh, R Kumazawa, I Seki, K Saito, Y Torii, Y P Zhao, D Hartmann, H Idei, S Kubo, K Ohkubo, M Sato, T Shimozuma, Y Yoshimura, K Ikeda, O Kaneko, Y Oka, M Osakabe, Y Takeiri, K Tsumori, N Ashikawa, P C deVries, M Emoto, A Fukuyama, H Funaba, M Goto, K Ida, S Inagaki, N Inoue, M Isobe, K Itoh, S Kado, K Kawahata, T Kobuchi, K Khlopenkov, A Komori, A Krasilnikov, Y Liang, S Masuzaki, K Matsuoka, I Minami, J Miyazawa, T Morisaki, S Morita, S Murakami, S Muto, Y Nagayama, Y Nakamura, H Nakanishi, K Narihara, K Nishimura, N Noda, A TNotake, S Ohdachi, N Ohyabu, H Okada, M Okamoto, T Ozaki, R O Pavlichenko, B J Peterson, A Sagara, S Sakakibara, R Sakamoto, H Sasao, M Sasao, K Sato, S Satoh, T Satow, M Shoji, S Sudo, H Suzuki, M Takechi, N Tamura, S Tanahashi, K Tanaka, K Toi, T Tokuzawa, K Y Watanabe, T Watanabe, H Yamada, I Yamada, S Yamaguchi, S Yamamoto, K Yamazaki, M Yokoyama, Y Hamada, O Motojima, M Fujiwara,
The Performance of ICRF Heated Plasmas in LHD, Sep 2000
(IAEA-CN-77/EX8/4)

NIFS-661 K Yamazaki, K Y Watanabe, A Sagara, H Yamada, S Sakakibara, K Narihara, K Tanaka, M Osakabe, K Nishimura, O Motojima, M Fujiwara, the LHD Group,
Helical Reactor Design Studies Based on New Confinement Scalings, Sep 2000
(IAEA-CN-77/ FTP 2/12)

NIFS-662 T Hayashi, N Mizuguchi, H Miura and T Sato,
Dynamics of Relaxation Phenomena in Spherical Tokamak, Sep 2000
(IAEA-CN-77THP2/13)

NIFS-663 H Nakamura and T Sato, H Kambe and K Sawada and T Saiki,
Design and Optimization of Tapered Structure of Near-field Fiber Probe Based on FDTD Simulation, Oct 2000

NIFS-664 N Nakajima,
Three Dimensional Ideal MHD Stability Analysis in $L=2$ Heliotron Systems, Oct 2000

NIFS-665 S Fujiwara and T Sato,
Structure Formation of a Single Polymer Chain I Growth of trans Domains, Nov 2000

NIFS-666 S Kida,
Vortical Structure of Turbulence, Nov 2000

NIFS-667 H Nakamura, S Fujiwara and T Sato,
Rigidity of Orientationally Ordered Domains of Short Chain Molecules, Nov 2000

NIFS-668 T Mutoh, R Kumazawa, T Seki, K Saito, Y Torii, F Shimpo, G Nomura, T Watari, D A Hartmann, M Yokota, K. Akaishi, N Ashikawa, P. deVries, M Emoto, H Funaba, M Goto, K Ida, H Idei, K Ikeda, S Inagaki, N Inoue, M Isobe, O Kaneko, K Kawahata, A Komori, T Kobuchi, S Kubo, S Masuzaki, T Morisaki, S Morita, J Miyazawa, S Murakami, T Minami, S Muto, Y Nagayama, Y Nakamura H Nakanishi, K Narihara, N Noda, K Nishimura, K Ohkubo, N Ohyabu, S Ohdachi, Y. Oka, M Osakabe, T Ozaki, B.J Peterson, A Sagara, N Sato, S Sakakibara, R Sakamoto, H Sasao, M Sasao, M Sato, T Shimozuma, M Shoji, S Sudo, H Suzuki, Y Takeiri, K Tanaka, K Toi, T Tokuzawa, K. Tsumori, K Y Watanabe I. Watanabe, H Yamada, I Yamada, S Yamaguchi, K. Yamazaki, M Yokoyama, Y Yoshimura, Y Hamada, O Motojima, M Fujiwara,
Fast- and Slow-Wave Heating of Ion Cyclotron Range of Frequencies in the Large Helical Device, Nov 2000

NIFS-669 K Mima, M S Jovanovic, Y Sentoku, Z-M Sheng, M M Skoric and T Sato,
Stimulated Photon Cascade and Condensate in Relativistic Laser-plasma Interaction, Nov 2000

NIFS-670 L Hadzievski, M M Skoric and T Sato,
On Origin and Dynamics of the Discrete NLS Equation, Nov 2000

NIFS-671 K Ohkubo, S Kubo, H Idei, T Shimozuma, Y Yoshimura, F Leuterer, M Sato and Y Takita,
Analysis of Oversized Sliding Waveguide by Mode Matching and Multi-Mode Network Theory, Dec 2000

NIFS-672 C. Das, S Kida and S Goto,
Overall Self-Similar Decay of Two-Dimensional Turbulence, Dec 2000

NIFS-673 L A Bureyeva, T Kato, V S Lisitsa and C Namba,
Quasiclassical Representation of Autoionization Decay Rates in Parabolic Coordinates, Dec 2000

NIFS-674 L A Bureyeva, V.S Lisitsa and C Namba,
Radiative Cascade Due to Dielectronic Recombination, Dec 2000

NIFS-675 M F.Heyn, S V Kasilof, W Kernbichler, K. Matsuoka, V V Nemov, S Okamura, O S Pavlichenko,
Configurational Effects on Low Collision Plasma Confinement in CHS Heliotron/Torsatron, Jan 2001

NIFS-676 K Itoh,
A Prospect at 11th International Toki Conference - Plasma physics, quo vadis?, Jan 2001

NIFS-677 S Satake, H Sugama, M Okamoto and M Wakatani,
Classification of Particle Orbits near the Magnetic Axis in a Tokamak by Using Constants of Motion, Jan 2001

NIFS-678 M Tanaka and A Yu Grosberg,
Giant Charge Inversion of a Macroion Due to Multivalent Counterions and Monovalent Coions Molecular Dynamics Studyn, Jan 2001

NIFS-679 K Akaishi, M Nakasuga, H Suzuki, M Iima, N Suzuki, A Komori, O Motojima and Vacuum Engineering Group,
Simulation by a Diffusion Model for the Variation of Hydrogen Pressure with Time between Hydrogen Discharge Shots in LHD, Feb 2001

NIFS-680 A Yoshizawa, N Yokoi, S Nisizima, S -I Itoh and K. Itoh
Variational Approach to a Turbulent Swirling Pipe Flow with the Aid of Helicity, Feb. 2001